

Nonlinear stochastic discrete drift-diffusion theory of charge fluctuations and domain relocation times in semiconductor superlattices

L. L. Bonilla,^{1,*} O. Sánchez,^{2,†} and J. Soler^{2,‡}

¹*Departamento de Matemáticas, Escuela Politécnica Superior, Universidad Carlos III de Madrid, Avenida de la Universidad 30, 28911 Leganés, Spain*

and Unidad Asociada al Instituto de Ciencia de Materiales (CSIC), 28049 Cantoblanco, Spain

²*Departamento de Matemática Aplicada, Facultad de Ciencias, Universidad de Granada, 18071 Granada, Spain*

(Received 27 December 2001; published 26 April 2002)

A stochastic discrete drift-diffusion model is proposed to account for the effects of shot noise in weakly coupled, highly doped semiconductor superlattices. Their current-voltage characteristics consist of a number of stable branches corresponding to electric field profiles displaying two domains separated by a domain wall. If the initial state corresponds to a voltage on the middle of a stable branch and is suddenly switched to a final voltage corresponding to the next branch, the domains relocate after a certain delay time. Shot noise causes the distribution of delay times to change from a Gaussian to a first passage time distribution as the final voltage approaches that of the end of the first current branch. These results agree qualitatively with experiments by Rogozia *et al.* [Phys. Rev. B **64**, 041308(R) (2001)].

DOI: 10.1103/PhysRevB.65.195308

PACS number(s): 05.40.-a, 73.50.Fq, 73.61.Ey, 05.45.-a

I. INTRODUCTION

The current-voltage (I - V) characteristics of highly doped weakly coupled semiconductor superlattices (SL's) typically exhibit many sharp branches due to the formation of static electric field domains.¹ Two branches are separated by a discontinuity in the current. The electric field profile associated with a given branch consists of two regions of constant electric field (domains) separated by a charge accumulation layer (domain boundary), which is confined to one or several quantum wells. The location of the domain boundary distinguishes I - V branches: as the voltage increases, the domain boundary is located closer to the injecting contact and the high-field domain increases at the expense of the low-field one.² Branches exhibit hysteresis cycles due to the coexistence of two or more stable electric field profiles at a given value of the voltage. Many interesting dynamical phenomena are associated with these SL's: (i) response of the SL's to sudden changes in bias (which may force relocation of electric field domains,³⁻⁶) and (ii) self-sustained oscillations of the current provided the temperature is raised or doping is lowered.^{7,8} Motivated by recent experimental evidence,^{9,10} we shall present in this paper a stochastic theory of domain relocation in highly doped SL's.

In relocation experiments,^{5,9,11} a doped SL displaying a multistable I - V characteristic is biased (typically) on the first plateau—say, in the middle of a branch. The corresponding field configuration has two domains separated by a domain wall which is an accumulation layer. Then the voltage is suddenly increased from V_0 to $V_1 = V_0 + \Delta V$ and the time evolution of the current is recorded. Depending on ΔV , the domain wall has to relocate so that a stable field configuration appropriate to the new voltage is reached.⁵ The outcome has been studied numerically using a discrete resonant tunneling model with Ohmic boundary conditions.⁶ For any $\Delta V < 0$ as well as for small positive ΔV , the relocation of the domain wall always occurs by a direct movement of the charge monopole forming the domain boundary to its final

position. This movement may be either upstream or downstream the electron flow as needed. However, for sufficiently large $\Delta V > 0$, a charge dipole is injected at the emitter contact in addition to the existing monopole, because the latter cannot move upstream beyond one SL period without encountering a stable field configuration.⁶ Recent experiments by Rogozia *et al.*¹¹ confirm this theoretical picture. Other experiments have shown that the relocation time for up jumps ($\Delta V > 0$) close to the discontinuity in the I - V characteristic is random and have also investigated its probability distribution function.^{9,10} What is causing randomness in the relocation time? In this paper we argue in favor of shot noise.

Shot noise occurring during a transport process is due to fluctuations in the occupation number of states caused by (i) thermal random initial fluctuations and (ii) the random nature of quantum-mechanical transmission and reflection (partition noise). The latter is in turn caused by the discrete nature of the electric charge.

The rest of the paper is organized as follows. In Sec. II, we derive a stochastic discrete drift-diffusion (DDD) model from the previously studied deterministic one (see Ref. 12) considering only partition noise (thermal noise is negligible in the low-temperature limit). The stochastic DDD model has multiplicative white noise terms obeying Poissonian statistics and it has been solved numerically by means of a second-order scheme proposed by Platen (Ref. 16, page 485). The results of numerically solving the stochastic model are reported in Sec. III. Our numerical results agree qualitatively with the experiments of Rogozia *et al.*,⁹ thereby enforcing the idea that shot noise is responsible for the observed fluctuations in domain relocation time. Details of the numerical scheme and comparison to rougher schemes and to the results of solving the deterministic model with random initial conditions are contained in the Appendix.

II. STOCHASTIC DISCRETE DRIFT-DIFFUSION MODEL

In weakly coupled SL's, typically the scattering times are much shorter than the escape times from quantum wells. In

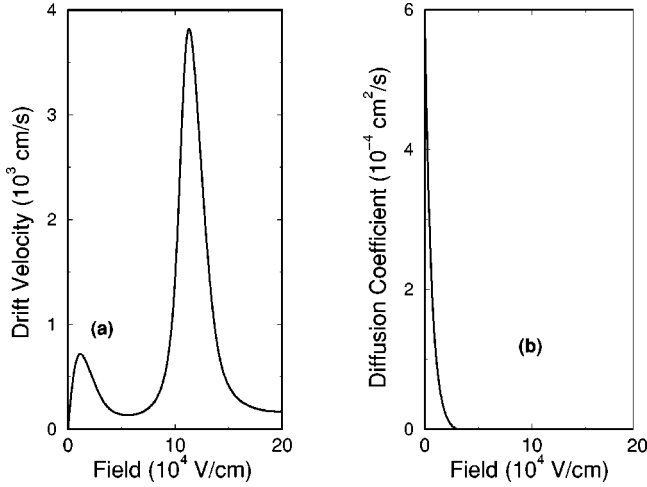


FIG. 1. Drift velocity and diffusion coefficient corresponding to the 9/4 GaAs/AIAs SL of Ref. 7.

their turn, the latter are shorter than typical dielectric relaxation times. This implies that the dominant mechanism of vertical charge transport is sequential resonant tunneling and that the tunneling current across barriers can be considered to be stationary. An appropriate discrete model consists of the Poisson and charge continuity equations for the two-dimensional (2D) electron density n_i and average electric field F_i at each SL period:²

$$F_i - F_{i-1} = \frac{e}{\epsilon} (n_i - N_D^w), \quad i = 1, \dots, N, \quad (1)$$

$$\frac{dn_i}{dt} = J_{i-1 \rightarrow i} - J_{i \rightarrow i+1}, \quad i = 1, \dots, N. \quad (2)$$

Here N_D^w , ϵ , and $eJ_{i \rightarrow i+1}$ are the 2D doping density at the i th well, the average permittivity of the SL, and the tunneling current density across the i th barrier, respectively.¹² We can differentiate Eq. (1) with respect to time and eliminate n_i by using Eq. (2). The result can be written as a form of Ampère's law for the balance of the current:

$$\frac{\epsilon}{e} \frac{dF_i}{dt} + J_{i \rightarrow i+1} = J(t). \quad (3)$$

Here $eJ(t)$ is the total current density through the SL's, equal for all SL periods, and $\epsilon dF_i/dt$ is the displacement current at the i th SL period. To have a closed system of equations, we need a constitutive relation linking $eJ_{i \rightarrow i+1}$ to the unknowns n_i and F_i . For a weakly coupled SL the stationary sequential tunneling current has been calculated by the transfer matrix Hamiltonian method¹³ or by the Green function formalism.¹⁴ In both cases, for sufficiently high temperature $J_{i \rightarrow i+1}$ may be approximated by a discrete drift-diffusion law $J_{i \rightarrow i+1}^{(d)} = n_i v(F_i)/l - D(F_i) (n_{i+1} - n_i)/l^2$.¹² The SL period is l and the electron drift velocity $v(F)$ and the diffusion coefficient $D(F_i)$ have the forms depicted in Fig. 1. In our numerical calculations, we have used parameters corresponding to the 9/4 SL of Ref. 7 at a temperature of 5 K. The three first subbands have energies of 44, 180, and 410 meV, re-

spectively, and we assume that the spectral functions of the wells are Lorentzians with half-widths of 10 meV.

The DDD model given by Eqs. (1) and (3) and $J_{i \rightarrow i+1} = J_{i \rightarrow i+1}^{(d)}$ has a conceptual difficulty coming from charge quantization that motivates the introduction of shot noise terms. The electric charge in each SL period, $e_A(n_i - N_D^w)$ (A is the SL cross section), should be a multiple of the electron charge e . This implies that the true charge fluctuates about the mean value given by the deterministic DDD model. To analyze charge fluctuations, we may use the Langevin ideas and add an appropriate stochastic term to $J_{i \rightarrow i+1}^{(d)}$. The SL cross section A is very large (a circular cross section of diameter 120 μm wide as compared to a SL period of $l = 13$ nm) and the barrier transmission coefficient is very small. Then we may use the classic Poissonian shot noise to model charge fluctuations:¹⁵

$$J_{i \rightarrow i+1} = \frac{n_i v^{(f)}(F_i) - n_{i+1} v^{(b)}(F_i)}{l} + J_{i \rightarrow i+1}^{(r)}(t), \quad (4)$$

for $i = 1, \dots, N-1$, where $J_{i \rightarrow i+1}^{(r)}$ represents the random current which satisfies

$$\langle J_{i \rightarrow i+1}^{(r)} \rangle = 0, \quad (5)$$

$$\langle J_{i \rightarrow i+1}^{(r)}(t) J_{j \rightarrow j+1}^{(r)}(t') \rangle = \delta_{ij} \delta(t-t') (Al)^{-1} [n_i v^{(f)}(F_i) + n_{i+1} v^{(b)}(F_i)], \quad (6)$$

and $v^{(b)}$, $v^{(f)}$ are defined as follows:

$$v^{(b)}(F) = \frac{D(F)}{l}, \quad v^{(f)}(F) = v^{(b)}(F) + v(F). \quad (7)$$

The logic behind this form of random tunneling current is as follows. We consider that uncorrelated electrons are arriving at the i th barrier with a distribution function of time intervals between arrival times that is Poissonian.¹⁵ Then the shot noise spectrum for the current $eJ_{i \rightarrow i+1}^{(r)} A$ is given by the average current $[n_i v^{(f)}(F_i) + n_{i+1} v^{(b)}(F_i)] e^2 A/l$, which in turn yields Eq. (6). As remarked in Ref. 15, this procedure assumes low transmission through the barriers and it yields an upper bound for the shot noise amplitude. In addition, the tunneling current is approximated by a discrete drift-diffusion expression whose transport coefficients (drift velocity, diffusivity, . . .) will be quantitatively different from those of the actual sample used in experiments. Given the exponential dependence of several quantities, relatively small differences in the location of extrema of the drift velocity, etc., may produce substantial differences. Thus, the mathematical model provides quantitative differences in the results but it yields the correct qualitative behavior.

The special nature of the emitter and collector layers is considered in the boundary conditions, given by Eq. (3) with $i=0$ and $i=N$ and different constitutive relations for the tunneling currents:¹²

$$J_{0 \rightarrow 1} = j_e^{(f)}(F_0) - \frac{n_1 w^{(b)}(F_0)}{l} + J_{0 \rightarrow 1}^{(r)}, \quad (8)$$

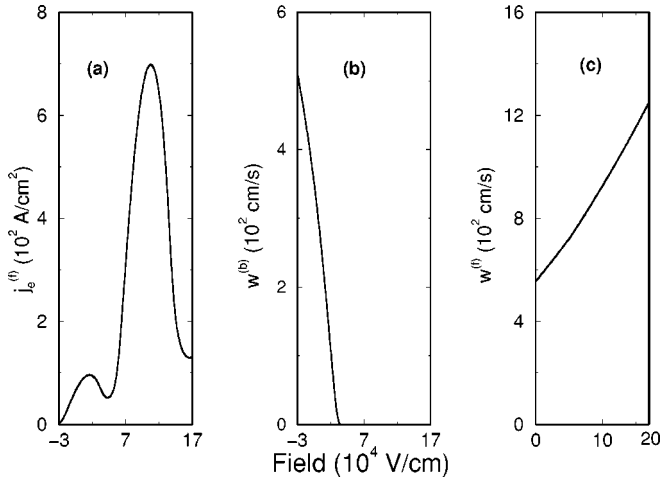


FIG. 2. Current-field contact characteristics corresponding to the 9/4 GaAs/AlAs SL of Ref. 7.

$$J_{N \rightarrow N+1} = \frac{n_N w^{(f)}(F_N)}{l} + J_{N \rightarrow N+1}^{(r)}. \quad (9)$$

Here we still have $\langle J_{i \rightarrow i+1}^{(r)} \rangle = 0$ for $i=0$ and $i=N$, while the correlations are

$$\langle J_{0 \rightarrow 1}^{(r)}(t) J_{0 \rightarrow 1}^{(r)}(t') \rangle = \frac{j_e^{(f)}(F_0) l + n_1 w^{(b)}(F_0)}{Al} \delta(t-t'), \quad (10)$$

$$\langle J_{N \rightarrow N+1}^{(r)}(t) J_{N \rightarrow N+1}^{(r)}(t') \rangle = \frac{n_N w^{(f)}(F_N)}{Al} \delta(t-t'). \quad (11)$$

The emitter current density $e j_e^{(f)}$, the emitter backward velocity $w^{(b)}$, and the collector forward velocity $w^{(f)}$ are functions of the electric field depicted in Fig. 2.¹²

In addition to the boundary conditions, the Ampère and Poisson equations should be supplemented with the voltage bias condition

$$\sum_{i=1}^N F_i l = V, \quad (12)$$

where V denotes voltage. Equations (1), (3), and (4)–(12) form a closed system of stochastic equations for n_i , F_i , and J . They constitute the stochastic DDD model. To analyze this model, it is convenient to render all equations dimensionless. Let us denote by (F_M, v_M) the coordinates of the first positive maximum of the drift velocity $v(F)$. We adopt F_M , N_D^w , v_M , $v_M l$, $e N_D^w v_M / l$, and $\varepsilon F_M l / (e N_D^w v_M)$ as units of F_i , n_i , $v(F)$, $D(F)$, eJ , and t , respectively. According to the parameters of the superlattice previously referred to, we find $F_M = 11.60$ kV/cm, $N_D^w = 1.5 \times 10^{11}$ cm⁻², $v_M = 718$ cm/s, $v_M l = 9.33 \times 10^{-4}$ cm²/s, and $e N_D^w v_M / l = 13.27$ A/cm². For a circular sample with a diameter of 120 μ m, the units of current and time are 1.501 mA and 1.021 ns, respectively. Then Eqs. (1), (3), and (4)–(12) become

$$E_i - E_{i-1} = v(n_i - 1), \quad (13)$$

$$J(t) = \frac{dE_i}{dt} + n_i v_i - D_i(n_{i+1} - n_i) + a \sqrt{n_i(v_i + D_i) + D_i n_{i+1}} \xi_i(t), \quad (14)$$

$$J(t) = \frac{dE_0}{dt} + J_e(E_0) - W_e(E_0) n_1 + a \sqrt{J_e(E_0) + W_e(E_0) n_1} \xi_0(t), \quad (15)$$

$$J(t) = \frac{dE_N}{dt} + W_c(E_N) n_N + a \sqrt{W_c(E_N) n_N} \xi_N(t), \quad (16)$$

$$\phi = \frac{1}{N} \sum_{i=1}^N E_i. \quad (17)$$

Here we have used the same symbols for dimensional and dimensionless quantities except for the electric field and the coefficient functions in the boundary conditions. The parameters $v = e N_D^w / (\varepsilon F_M) \approx 1.772$, $\phi = V / (F_M N l)$, and $a = \sqrt{e / (\varepsilon F_M A)} \approx 3.232 \times 10^{-4}$ are the dimensionless doping, the average electric field (bias), and the noise amplitude, respectively. $\xi_i(t)$ is a zero-mean Gaussian white noise with correlation $\langle \xi_i(t) \xi_j(t') \rangle = \delta_{ij} \delta(t-t')$ [$\xi_i(t) = \xi_i(t_m) / \sqrt{\Delta t}$, where the $\xi_i(t_m)$ are independent identically distributed (i.i.d.) normalized Gaussian random variables for each discrete time t_m and Δt is the dimensionless time step]. The rest of the coefficients in Eqs. (13)–(16) are defined by

$$v_i \equiv v(E_i) = \frac{v(F_M E_i)}{v_M},$$

$$D_i \equiv D(E_i) = \frac{D(F_M E_i)}{V_M l},$$

$$J_e(E_0) = \frac{j_e^{(f)}(F_M E_0) l}{N_D^w v_M},$$

$$W_e(E_0) = \frac{W^{(b)}(F_M E_0)}{v_M},$$

$$W_c(E_N) = \frac{W^{(f)}(F_M E_N)}{v_M}. \quad (18)$$

The previous system of equations can be further simplified since the electron densities n_i and the total current density $J(t)$ can be expressed in terms of the electric field and the bias. Differentiating Eq. (17) with respect to time and using Eqs. (15) and (16), we obtain an expression for the total current density $J(t)$:

$$\begin{aligned} \frac{d\phi}{dt} &= \frac{1}{N} \sum_{i=1}^N \frac{dE_i}{dt} = J - \frac{1}{N} \sum_{i=1}^{N-1} [n_i(v_i + D_i) - n_{i+1}D_i] \\ &\quad - \frac{n_N W_c(E_N)}{N} - \frac{a}{N} \sum_{i=1}^{N-1} \sqrt{n_i v_i + (n_i + n_{i+1}) D_i} \xi_i(t) \\ &\quad - \frac{a}{N} \sqrt{n_N W_c(E_N)} \xi_N(t). \end{aligned}$$

Then the total current can be written as

$$J = J_1 + \mathbf{J}_2 \cdot \boldsymbol{\xi}, \quad (19)$$

$$J_1 = \frac{d\phi}{dt} + \sum_{i=1}^{N-1} \frac{n_i(v_i + D_i) - n_{i+1}D_i}{N} + \frac{n_N W_c(E_N)}{N}, \quad (20)$$

$$(\mathbf{J}_2)_0 = 0, \quad (21)$$

$$(\mathbf{J}_2)_i = \frac{a \sqrt{n_i v_i + (n_i + n_{i+1}) D_i}}{N}, \quad 1 \leq i < N, \quad (22)$$

$$(\mathbf{J}_2)_N = \frac{a \sqrt{n_N W_c(E_N)}}{N}, \quad (23)$$

$$\boldsymbol{\xi} = (\xi_0(t), \dots, \xi_N(t))^T. \quad (24)$$

We can now insert these equations into the Ampère Eqs. (14)–(16) and eliminate n_i by using Eq. (13), thereby obtaining a stochastic differential equation of the following form:

$$\frac{d\mathbf{E}}{dt} = \mathbf{H} \left(\mathbf{E}, \frac{d\phi}{dt} \right) + S(\mathbf{E}) \cdot \boldsymbol{\xi}(t), \quad (25)$$

for the $(N+1)$ -dimensional vector electric field $\mathbf{E} = (E_0, \dots, E_N)^T$. Here $S(\mathbf{E})$ is a $(N+1) \times (N+1)$ matrix and \mathbf{H} is a $(N+1)$ -dimensional vector having obvious forms which we do not write explicitly for the sake of conciseness.

The stochastic differential equation (25) has been numerically solved by using two different methods: a first order

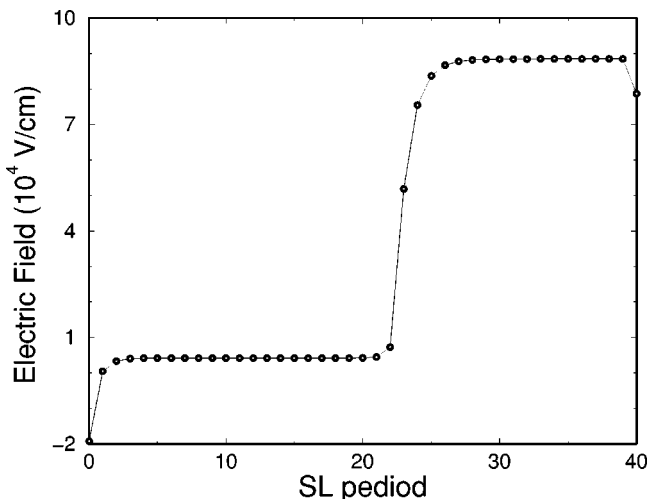


FIG. 3. Static electric field profile at $V=2.1$ V.

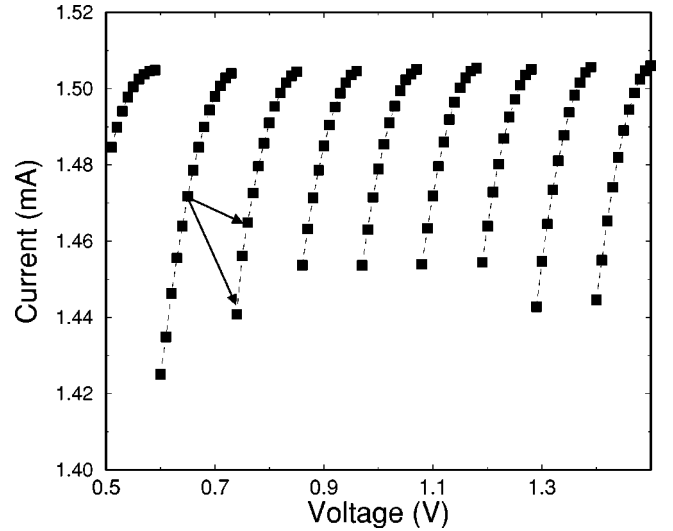


FIG. 4. Part of the first plateau of the I - V characteristics.

Heun scheme (modified Euler scheme) and the second-order scheme proposed by Platen.¹⁶ The second numerical scheme is rather more costly, but we had to use it to avoid that numerical errors mask the effects due to charge fluctuations. Technical details on numerical schemes and a comparison of their performances are given in the Appendix. The results of our simulations are reported in the next section.

III. NUMERICAL RESULTS

We have numerically investigated the sample of Ref. 7 that was used in the relocation experiments.^{5,9} It consists of a $N=40$ period SL with 9-nm-wide GaAs wells and 4-nm-wide AlAs barriers, and 2D doping $N_D^w = 1.5 \times 10^{11} \text{ cm}^{-2}$, at a temperature $T=5$ K. We have solved numerically the non-dimensional equations in the units and dimensionless parameters introduced in Sec. II.

Figures 3 and 4 show a typical static electric field profile

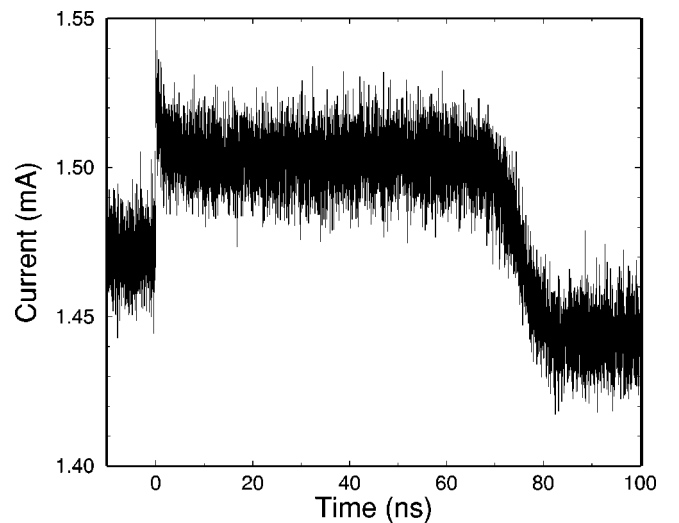


FIG. 5. Time trace of the current when the voltage is switched from $V_0=0.65$ V to $V_f=0.737$ V.

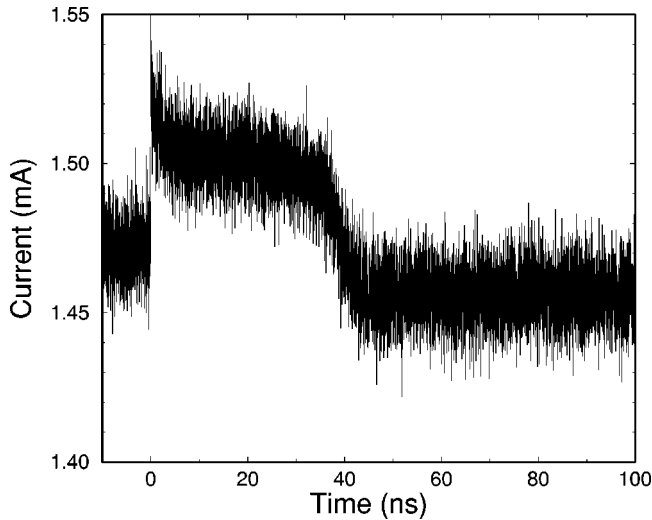


FIG. 6. As in Fig. 5, but with a final voltage $V_f=0.75$ V.

(with two coexisting domains) and the first plateau of the time-averaged $I-V$ characteristics (obtained by voltage up-sweeping). To ascertain the influence of charge fluctuations in domain relocation, we start by setting a stationary field configuration corresponding to a voltage $V_0=0.65$ V on the lower branch of Fig. 4. At time $t=0$, the voltage increases (in one time step) to its final value V_f on the next $I-V$ branch.

Time traces of the current are depicted in Figs. 5–7. Notice that the vertical scale has been augmented sufficiently to see the fluctuations of the current, which are typically about 0.02 in size. To compare our numerical results to experimental ones, we need to characterize the domain relocation times and their distribution function. After a voltage switch, each realization of the random solution of Eq. (25) gives rise to jumps in the mean current as depicted in Figs. 5–7. We compare the time trace of the current (time averaged over intervals of five time dimensionless units) to the value of the current in static $I-V$ branches. The first time t_0 that the current time trace differs less than 5×10^{-4} dimensionless units from its final stationary value, we consider that the domain

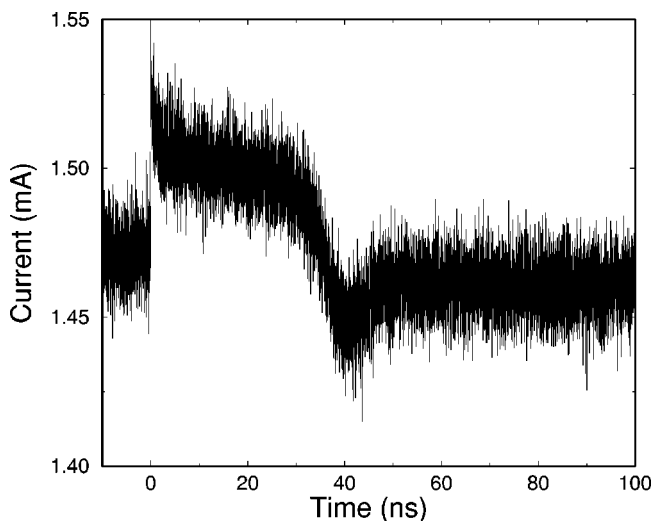


FIG. 7. As in Fig. 5, but with a final voltage $V_f=0.755$ V.

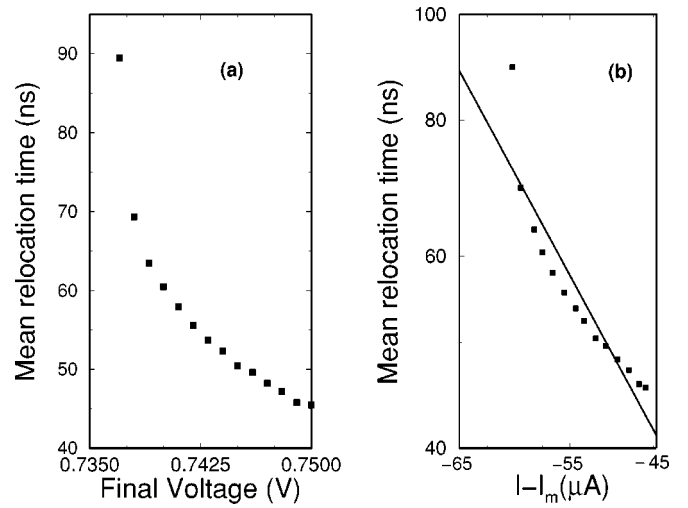


FIG. 8. (a) Mean relocation time for different final voltages. (b) Logarithm of the mean delay time vs current difference between final current and the maximum or minimum current I_m of the initial branch.

relocation has ended. The distribution of time delays t_0 taken over many realizations is then recorded. For a large voltage switch, the time delay before the current falls from its initial value to its final level is shorter than for a smaller voltage switch; compare Figs. 5 and 6. The differences between the time delays involved in these two cases (about 40 ns) are smaller than those recorded in experiments.⁹ These differences occur because of overestimation of the field F_M and the shot noise amplitude by our theoretical calculations with respect to those of the experimental sample, as we mentioned before.

In Ref. 5 it was claimed that the time delay depends exponentially on the difference between the final value of the stabilized current I and the maximum value of the current (or minimum value in the case of a down switch) at the initial

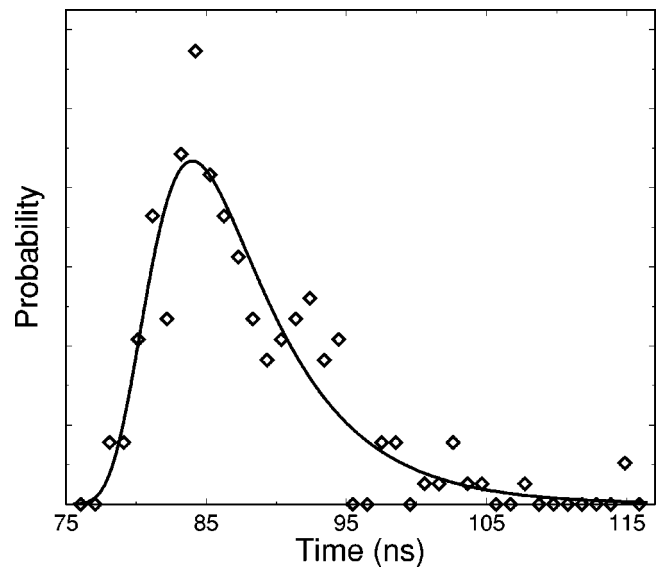


FIG. 9. Time delay distribution for $V_f=0.737$ V. Data from numerical simulations have been fitted to a FPT distribution.

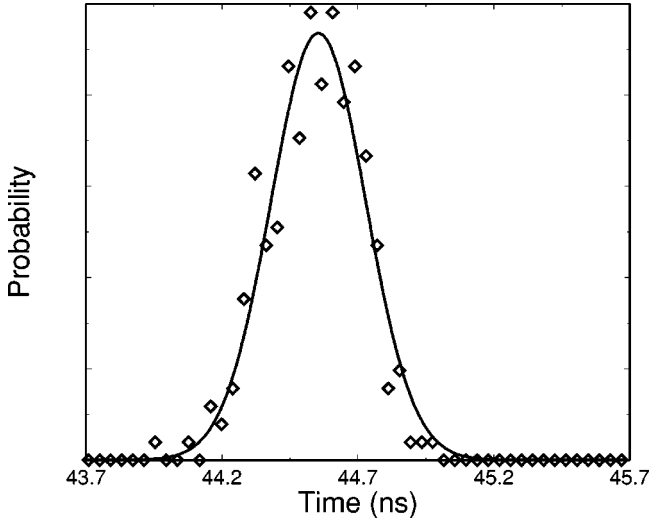


FIG. 10. Time delay distribution for $V_f=0.75$ V. Data from numerical simulations have been fitted to a Gaussian distribution.

branch, I_m . Then the relocation time (measured in units of 1.021 ns) depends exponentially on the current difference $I - I_m$, i.e.,

$$\exp\left(\frac{b|I - I_m|}{I_M} + c\right). \quad (26)$$

We have observed this dependence in our numerical results too. The dimensionless constants b and c are $b = 64.9866$ and $c = 1.6717$. Here $I_M = 1.501$ mA is the unit of current. In the experiments of Luo *et al.*,⁵ $I_M = 136$ μ A (approximately the height of the first maximum of the current in the inset of Fig. 1), $b = 10.74$ (6 times smaller than the numerically calculated value), and $c = 3.34$ (2 times larger than the numerically calculated value). We thus confirm the exponential dependence of the relocation time on the current difference and observe a good qualitative agreement between numerically and experimentally obtained values.

Figure 8(a) shows the mean relocation time obtained in our simulations as a function of V_f . As the final voltage approaches that corresponding to I_M , the relocation time increases. Figure 8(b) depicts the mean relocation time as a function of $(I - I_m)$ on a semilogarithmic scale for V_f values between 0.737 and 0.735 V. The solid line denotes a linear fit to the data points, which agrees with the exponential law proposed by Luo *et al.*⁵ These figures are qualitatively similar to the corresponding ones depicted from experimental

TABLE I. Descriptive statistics of the relocation time distributions obtained with the Heun scheme.

Heun	$V_f=0.737$	$V_f=0.75$
Lower limit (ns)	77.692	43.775
Upper limit (ns)	128.048	45.633
Mean (ns)	87.863	44.564
Standard deviation (ns)	6.803	0.299
Skewness coeff.	1.840	0.131

TABLE II. Descriptive statistics of the relocation time distributions obtained with the Platen scheme.

Platen	$V_f=0.737$	$V_f=0.75$
Lower limit (ns)	77.827	43.942
Upper limit (ns)	115.025	44.960
Mean (ns)	87.635	44.541
Standard deviation (ns)	6.339	0.167
Skewness coeff.	1.4237	-0.2791

data in Refs. 9 and 5. Quantitative differences are due to the above-mentioned discrepancies in F_M , the tunneling current, and the shot noise amplitude. Now we focus on the distribution of switching times. Typically, delay distributions are either close to symmetric Gaussians or they are asymmetric, depending on how far V_f is from the limit point of the I - V characteristics. We have fitted our numerical distributions by least squares either to a Gaussian density:

$$W(t, \tau, \sigma) = \frac{1}{\sigma\sqrt{2\pi}} \exp\left(-\frac{(t-\tau)^2}{2\sigma^2}\right) \quad (27)$$

or to a first passage time (FPT) distribution

$$W(t, y, \beta) dt = \sqrt{y} \frac{2\beta}{\pi} \exp\left(-\frac{\beta y z^2}{2}\right) dz, \quad (28)$$

where

$$z = \frac{1}{\sqrt{\exp(2\beta t) - 1}}. \quad (29)$$

The parameters of these distributions are τ (mean relocation time) and σ (standard deviation) for the Gaussian and y and β for the FPT distribution. The results of our fitting are depicted in Figs. 9 and 10.

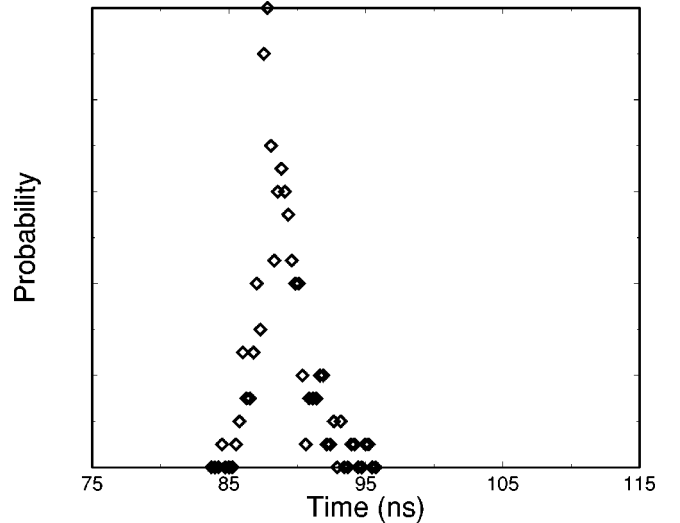


FIG. 11. Time delay distribution for $V_f=0.737$ calculated with a deterministic Heun scheme and random initial conditions.

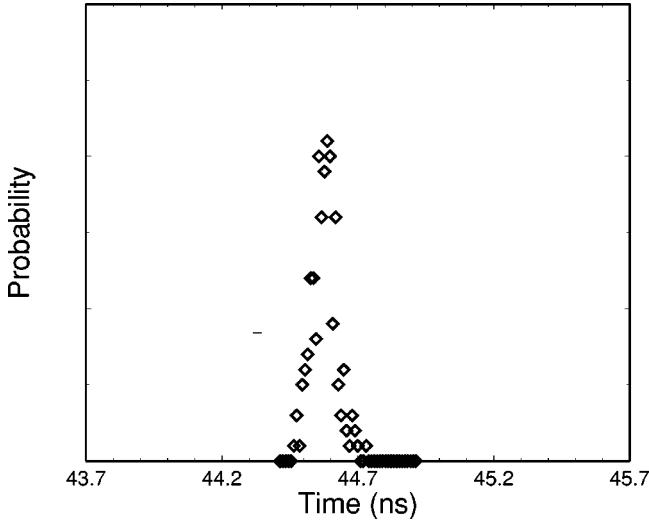


FIG. 12. Time delay distribution for $V_f=0.75$ calculated with a deterministic Heun scheme and random initial conditions.

These results agree qualitatively with the experimental ones of Rogozia *et al.*⁹ As in Ref. 9, our Figs. 9 and 10 show that for values of the voltage far away from the current jump the time delay distribution changes from an asymmetric FPT distribution to a very narrow symmetric Gaussian distribution as V_f departs from the voltage corresponding to the current jump. These features have a numerical expression in terms of descriptive statistics like the mean, the standard deviation, or the skewness coefficient as shown in the tables of the Appendix. The numerically calculated largest and smallest delay times are also presented.

APPENDIX: NUMERICAL SCHEME

This appendix is devoted to explain some technical details of the simulations. The Platen second-order scheme gives the vector field \mathbf{E}^{n+1} at discrete time $t + \Delta t$ as the following function of \mathbf{E}^n at discrete time t (Ref. 16):

$$\begin{aligned} \mathbf{E}^{n+1} = & \mathbf{E}^n + \frac{1}{2} \left[\mathbf{H} \left(\mathbf{Y}, \frac{d\phi}{dt} \right) + \mathbf{H} \left(\mathbf{E}^n, \frac{d\phi}{dt} \right) \right] \Delta t + \frac{1}{4} \sum_{j=1}^{N+1} \left[[\mathbf{S}^j(\mathbf{M}_+^j) + \mathbf{S}^j(\mathbf{M}_-^j) + 2\mathbf{S}^j(\mathbf{E}^n)] \Delta W^j + \sum_{r=1, r \neq j}^{N+1} [\mathbf{S}^j(\mathbf{U}_+^r) + \mathbf{S}^j(\mathbf{U}_-^r) \right. \\ & \left. - 2\mathbf{S}^j(\mathbf{E}^n)] \Delta W^j \right] + \frac{1}{4} \sum_{j=1}^{N+1} \left[[\mathbf{S}^j(\mathbf{M}_+^j) - \mathbf{S}^j(\mathbf{M}_-^j)] \{ (\Delta W^j)^2 - \Delta t \} + \sum_{r=1, r \neq j}^{N+1} [\mathbf{S}^j(\mathbf{U}_+^r) - \mathbf{S}^j(\mathbf{U}_-^r)] \{ \Delta W^j \Delta W^r + V_{r,j} \} \right]. \end{aligned}$$

Here $\mathbf{S}^j(\cdot)$ is the j th column of $\mathbf{S}(\cdot)$, $\mathbf{U}_\pm = \mathbf{E}^n \pm \mathbf{S}(\mathbf{E}^n)^j \sqrt{\Delta t}$, and \mathbf{H} and \mathbf{S} are evaluated at

$$\mathbf{Y} = \mathbf{E}^n + \mathbf{H} \left(\mathbf{E}^n, \frac{d\phi}{dt} \right) \Delta t + \sum_{j=1}^{N+1} \mathbf{S}(\mathbf{E}^n)^j \Delta W^j,$$

$$\mathbf{M}_\pm^j = \mathbf{E}^n + \mathbf{H} \left(\mathbf{E}^n, \frac{d\phi}{dt} \right) \Delta t \pm \mathbf{S}^j(\mathbf{E}^n) \sqrt{\Delta t}.$$

ΔW^j are independent Gaussian random variables distributed with zero mean and variance Δt , whereas the V_{j_1, j_2} are independent two point random variables that satisfy

TABLE III. Descriptive statistics of the relocation time distributions obtained with perturbed initial conditions.

	$V_f=0.737$	$V_f=0.75$
Mean (ns)	88.916	44.579
Standard deviation (ns)	1.773	0.045
Skewness coeff.	0.912	0.255

IV. CONCLUSIONS

We have studied how the shot noise due to charge quantization affects the relocation time of electric field domains after a sudden switch of the voltage. We find that the mean relocation time depends exponentially on the difference between the value of the current at the final voltage and the value of the current at the end of the branch corresponding to the initial voltage. The distribution function of delay times after a voltage switch changes from Gaussian to a FPT distribution as the final voltage approaches the limit point of the stationary I - V characteristics. These results are in qualitative agreement with experiments.

ACKNOWLEDGMENTS

We thank Dr. Guillermo Carpintero for fruitful discussions during the early stages of this work. We acknowledge financial support of the DGES Grant Nos. PB98-0142-C04-01 (L.L.B.) and PB98-1281 (O.S. and J.S.).

$$P(V_{j_1, j_2} = \pm \Delta t) = \frac{1}{2},$$

$$V_{j_1, j_1} = -\Delta t, \quad V_{j_1, j_2} = -V_{j_2, j_1}.$$

We have used a time step of $\Delta t = 10^{-4}$ (in dimensionless units) of the same order as the noise amplitude a . The values of the random variables V and W have been generated through a random number generator improved by using a seed selector depending on the computer clock and an algorithm which allows to avoid the sequential correlation usual

in this sort of generators.¹⁷ The Platen scheme is second-order weakly convergent in the following sense. Let $g(\mathbf{E})$ be any sufficiently smooth scalar function [with $2(\beta+1)$ continuous derivatives provided β is the order of the scheme]. Let us fix the time instant at t corresponding to discrete time n . Then

$$|\langle g(\mathbf{E}^n) \rangle - \langle g(\mathbf{E}) \rangle| \leq C(\Delta t)^2,$$

for any $\Delta t \in (0, \delta_0)$, where C and δ_0 are positive constants. The Platen numerical scheme is certainly more complicated and costly than even a stochastic Heun (modified Euler) first-order scheme. We have had to use it to minimize the effects of numerical noise coming from floating-point arithmetic (even our high-precision 64-bit arithmetic) and that inherent in interpolating our transport coefficients and contact functions in the boundary conditions. In fact, in the absence of the noise, both the Heun and the Platen schemes become the well-known deterministic Heun (improved Euler) scheme—that is, a second-order Runge-Kutta method:

$$\mathbf{E}^{n+1} = \mathbf{E}^n + \frac{\Delta t}{2} [\mathbf{H}(\mathbf{E}^n) + \mathbf{H}(\mathbf{E}^n + \mathbf{H}(\mathbf{E}^n)\Delta t)].$$

However, both schemes differ in their treatment of the noise: the stochastic Heun method is weakly first order whereas the Platen scheme is second order. The result obtained by using the Platen scheme exhibits less dispersion than that reached by the Heun method, as shown in Tables I and II. An appropriate treatment of the noise term avoids the presence of artificial numerical effects. The effects of the numerical perturbations can be illustrated as follows. Let us use the deterministic Heun scheme with random initial conditions corresponding to disturbances of the stationary field profile at voltage V_0 and suddenly switch to voltage V_f . The domain relocation times have been measured and they give rise to the distributions of Figs. 11 and 12. We have compared the mean, standard deviation, and skewness coefficient¹⁸ of these distributions to those corresponding to the use of the stochastic Heun and Platen schemes; see Tables I, II, and III. Notice that the mean relocation times are similar, while the numerical viscosity contributes to scatter the results. The shot noise does not change the mean values given by the deterministic model, but the dispersion measured by the standard deviation increases due to numerical effects (larger in the Heun scheme). The use of a numerical scheme that reduces these effects is then clearly justified.

*Electronic address: bonilla@ing.uc3m.es

†Electronic address: ossanche@ugr.es

‡Electronic address: jsoler@ugr.es

¹H.T. Grahn, R.J. Haug, W. Müller, and K. Ploog, *Phys. Rev. Lett.* **67**, 1618 (1991).

²L. L. Bonilla, in *Nonlinear Dynamics and Pattern Formation in Semiconductors and Devices*, edited by F.-J. Niedernostheide (Springer, Berlin, 1995), Chap. 1.

³J. Kastrop, F. Prengel, H.T. Grahn, K. Ploog, and E. Schöll, *Phys. Rev. B* **53**, 1502 (1996).

⁴Y. Shimada and K. Hirakawa, *Jpn. J. Appl. Phys., Part 1* **36**, 1944 (1997).

⁵K.J. Luo, H.T. Grahn, and K.H. Ploog, *Phys. Rev. B* **57**, R6838 (1998).

⁶A. Amann, A. Wacker, L.L. Bonilla, and E. Schöll, *Phys. Rev. E* **63**, 066207 (2001).

⁷J. Kastrop, R. Hey, K.H. Ploog, H.T. Grahn, L.L. Bonilla, M. Kindelan, M. Moscoso, A. Wacker, and J. Galán, *Phys. Rev. B* **55**, 2476 (1997).

⁸D. Sánchez, L.L. Bonilla, and G. Platero, *Phys. Rev. B* **64**, 115311 (2001).

⁹M. Rogozia, S.W. Teitsworth, H.T. Grahn, and K.H. Ploog, *Phys. Rev. B* **64**, 041308 (2001).

¹⁰M. Rogozia, H. T. Grahn, S. W. Teitsworth, and K. H. Ploog, *Physica B* **314**, 427 (2002).

¹¹M. Rogozia, S. W. Teitsworth, H. T. Grahn, and K. H. Ploog, *Phys. Rev. B* (to be published).

¹²L.L. Bonilla, G. Platero, D. Sánchez, *Phys. Rev. B* **62**, 2786 (2000).

¹³R. Aguado, G. Platero, M. Moscoso, and L.L. Bonilla, *Phys. Rev. B* **55**, R16 053 (1997).

¹⁴A. Wacker, in *Theory of Transport Properties of Semiconductor Nanostructures*, edited by E. Schöll (Chapman and Hall, London, 1998), Chap. 10.

¹⁵Ya.M. Blanter and M. Büttiker, *Phys. Rep.* **336**, 1 (2000).

¹⁶P. E. Kloeden and E. Platen, *Numerical Solution of Stochastic Differential Equations* (Springer, Berlin, 1992).

¹⁷W. H. Press, B. P. Flannery, S. A. Teukolsky, and W. T. Vetterling, *Numerical Recipes in C: The Art of Scientific Computing* (Cambridge University Press, Cambridge, UK, 1988).

¹⁸The skewness (Fisher) coefficient measures the asymmetry of a distribution and is calculated as the distribution third central moment divided by the third power of its standard deviation.